AJNR

Susceptibility-Weighted Angiography for the Follow-Up of Brain Arteriovenous Malformations Treated with Stereotactic Radiosurgery

S. Finitsis, R. Anxionnat, B. Gory, S. Planel, L. Liao and S. Bracard

AJNR Am J Neuroradiol 2019, 40 (5) 792-797
doi: https://doi.org/10.3174/ajnr.A6053
http://www.ajnr.org/content/40/5/792

Susceptibility-Weighted Angiography for the Follow-Up of Brain Arteriovenous Malformations Treated with Stereotactic Radiosurgery

S. Finitsis, R. Anxionnat, B. Gory, S. Planel, L. Liao, and S. Bracard

ABSTRACT

SUMMARY: The criterion standard for assessing brain AVM obliteration postradiosurgery is DSA. To explore the value of susceptibility-weighted angiography, we followed 26 patients with brain AVMs treated by radiosurgery using susceptibility-weighted angiography and DSA. Studies were evaluated by 2 independent readers for residual nidi. Susceptibility-weighted angiography demonstrated good intermodality ($\kappa = 0.71$) and interobserver ($\kappa = 0.64$) agreement, and good sensitivity (85.7%) and specificity (85.7%). Susceptibility-weighted angiography is a useful radiation- and contrast material–free technique to follow-up brain AVM obliteration postradiosurgery.

ABBREVIATIONS: bAVM = brain AVM; SRS = stereotactic radiosurgery; SWAN = susceptibility-weighted angiography

Brain AVMs (bAVMs) may be treated by either surgical resection, embolization, or radiosurgery. Following treatment, confirmation of complete obliteration is imperative because the risk of bleeding in incompletely obliterated lesions persists.[1-3] After AVM radiosurgery, occlusion is usually achieved after 2–4 years, with regular imaging follow-up performed every 6–12 months until complete bAVM obliteration is documented.[1,2]

The criterion standard for evaluating post-stereotactic radiosurgery (SRS) bAVM obliteration is DSA because of its high spatial and temporal resolution.[4,5] However, DSA is a high-cost, invasive procedure involving radiation and contrast media exposure, with a 1% morbidity.[6-9] Noninvasive alternatives such as 3D-TOF-MRA, 3D contrast-enhanced MRA,[10-12] and, lately, 4D time-resolved MRA[11,13,14] have shown inferior diagnostic accuracy compared to DSA. Moreover, most entail intravenous administration of contrast material with additional cost and potential toxicity.[15,16]

Susceptibility-weighted angiography (SWAN) is a promising new technology that indirectly evaluates the amount of oxygen within blood vessels. As bAVMs shunt oxygenated blood from arteries to veins, bAVM draining veins appear hyperintense,[17] while normal veins containing deoxygenated blood appear hypointense.[18,19] SWAN demonstrates high spatial resolution that allows small normal draining veins with a diameter inferior to the size of the voxel to be visualized and is highly sensitive to small, low-flow shunts.[19] Moreover, SWAN does not require administration of intravenous contrast material. We aimed to evaluate the performance of SWAN for the follow-up of patients with bAVMs treated with SRS.

MATERIALS AND METHODS

Inclusion Criteria

After institutional review board approval, all patients with bAVMs treated with SRS at the University Hospital of Nancy, France were prospectively included in a database. For the present study, patients imaged between March 2012 and May 2018 were included if they met the following criteria: 1) They had a bAVM treated by embolization and radiosurgery or radiosurgery only, 2) they were imaged during follow-up with SWAN at 1.5T or 3T and DSA, 3) both examinations were performed within a time interval of <6 months and without another treatment session in between, and 4) both examinations were performed at least 12 months after SRS.

The treatment strategy for each patient was based on multidisciplinary decisions involving neurosurgeons, radiotherapists, and neuroradiologists. For each patient, demographics, bleeding history, comorbidities, location of the nidus, Spetzler-Martin grade, previous treatment history, clinical symptoms, and radiosurgical parameters were recorded in a prospective database. The time intervals between SRS and SWAN imaging, SWAN imaging and DSA control were also recorded.

Imaging

After SRS treatment, each patient underwent clinical evaluation and MR imaging at 6-month intervals on either 1.5T or 3T scan-

Received December 17, 2018; accepted after revision March 10, 2019.

From the Department of Neuroradiology (R.A., B.G., S.P., L.L., S.B.), Centre Hospitalier Universitaire de Nancy, Nancy, France; and AHEPA Hospital (S.F.), Aristotle University of Thessaloniki, Thessaloniki, Greece.

Please address correspondence to Stephanos Finitsis, MD, AHEPA Hospital, Aristotle University of Thessaloniki, Thessaloniki, Greece; e-mail: stefanosfin@yahoo.com; @StephanosFinits

http://dx.doi.org/10.3174/ajnr.A6053

ners (Signa 1.5T and 3T; GE Healthcare, Milwaukee, Wisconsin). The MR imaging SWAN protocol was fairly consistent: At 1.5T, the SWAN scanning parameters were the following: flip angle, 12°; TE, 80 ms; TR, 78.3 ms; slice thickness, 2.4 mm; FOV, 24 cm. At 3T, the SWAN scanning parameters were the following: flip angle, 15°; TE, 25 ms; number of echoes, 6; TR, minimum; slice thickness, 0.8 mm reconstructed in 2-mm MIP; FOV, 24 cm. DSA was performed on a biplane angiography unit (Innova; GE Healthcare) with selective contrast injections of intracranial vessels in standard projections.

Image Analysis

Two independent senior readers (S.B. and R.A.), with >20 years of experience in diagnostic and interventional neuroradiology each, reviewed the axial SWAN examinations randomly and confirmed the presence or absence of a remaining arteriovenous shunt, that is, the presence of hypersignal within the nidus or a draining vein. Readers were blinded to baseline and follow-up clinical data, DSA imaging, bAVM location, and treatments received. In case of disagreement, consensus was reached by a third senior neuroradiologist (S.F.). Results were recorded separately and used to determine interobserver and intermodality agreement.

DSA studies were reviewed in consensus by 2 other senior readers. Total obliteration of the bAVM was defined as the complete absence of the nidus, normalization of the afferent and efferent vessels, and a normal circulation time. Any remaining nidus, regardless of its size, was considered "patent," including the existence of early-filling draining veins.

Statistical Analysis

Quantitative variables were described as median and interquartile ranges, whereas qualitative variables were described as numbers and percentages. Intermodality and interobserver agreement was calculated using the κ statistic. All analyses were completed using commercial statistical software (SPSS, Version 23.0; IBM, Armonk, New York).

RESULTS

Twenty-six patients fulfilled the inclusion criteria (Fig 1). Patient demographics are shown in Table 1. Two patients underwent 2 sets of imaging at different time points that were included in the analysis. Before SRS, 23 patients were embolized with a mixture of *n*-BCA and glue; and 1, with Onyx (Covidien, Irvine, California).

Interobserver Agreement

For SWAN examinations, the 2 observers agreed on the existence of a residual nidus in 23 of 28 cases (82.1%), resulting in good interobserver agreement ($\kappa = 0.64$; 95% CI, 0.36–0.92) (Figs 2 and 3). Table 2 shows the interpretations according to the 2 readers and the consensus reading. Two disagreements corresponded to nidus remnants of millimetric size. Three more disagreements corresponded to occluded nidi that contained faint hyperintense spots.

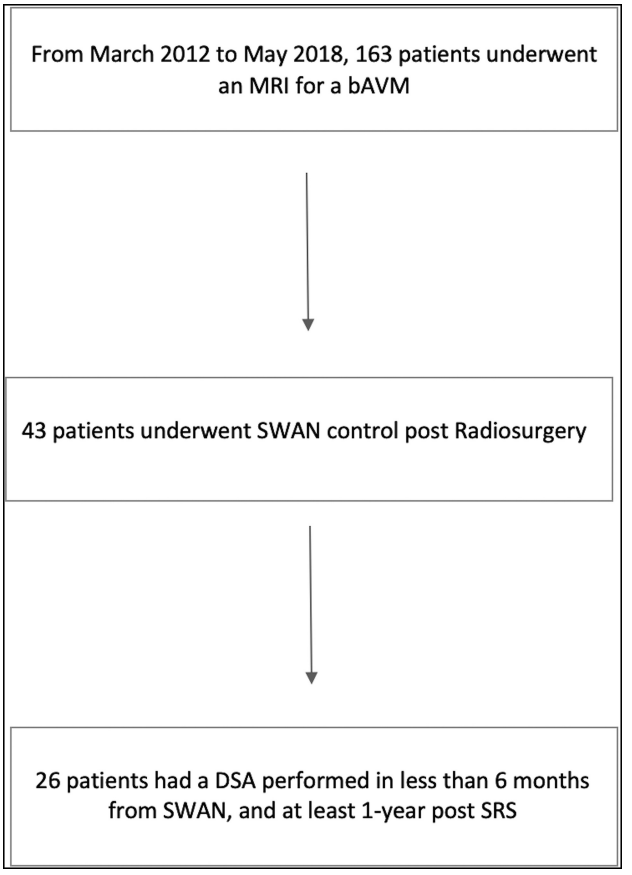

FIG 1. Patient flow chart.

Table 1: Characteristics of the 26 patients[a]

Characteristics	
Age (yr)	33 (22–42)
Sex, male	17 (65.4%)
bAVM location	
Supratentorial	24 (92.3%)
Infratentorial	2 (7.7%)
Spetzler-Martin grade	I (I–II)
Presentation	
Hemorrhage	20 (76.9%)
Seizure	4 (15.4%)
Headache	5 (19.2%)
Neurologic symptoms	1 (3.8%)
Type of treatment	
Embolization then radiosurgery	22 (84.6%)
Radiosurgery	2 (7.7%)
Surgery then embolization then radiosurgery	2 (7.7%)
Time intervals	
Delay between last treatment and SWAN (mo)[b]	34 (27.7–46.8)
Delay between SWAN and DSA (days)[b]	3 (3–65)

[a] Continuous variables are presented as proportion and percentage; categoric variables are described as median and first and third quartiles.
[b] Calculated for 28 datasets because 2 patients had 2 separate SWAN/DSA follow-ups.

Intermodality Agreement

The consensus reading for SWAN showed agreement regarding residual nidi in 24/28 (85.7%) cases, resulting in good intermodality agreement ($\kappa = 0.71$; 95% CI, 0.455–0.974). Two unseen nidi (false-negative cases) were very small (Fig 4). One false-positive case was due to a large intranidal calcification that was obvious on plain CT (Fig 5). Another false-positive case was a corpus

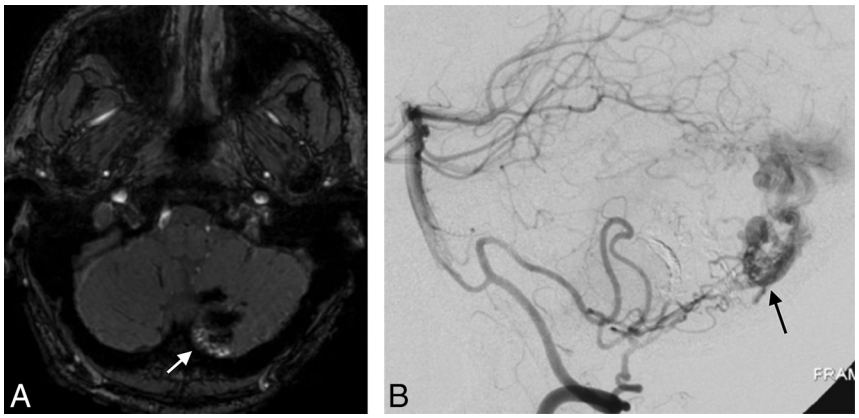

FIG 2. A 42-year-old man with a left cerebellar AVM, partially embolized with glue. *A*, SWAN imaging 3 years after SRS shows hyperintense vessels (*white arrow*) in the posterior part of the nidus that correspond to a nidal remnant confirmed by DSA (*black arrow, B*).

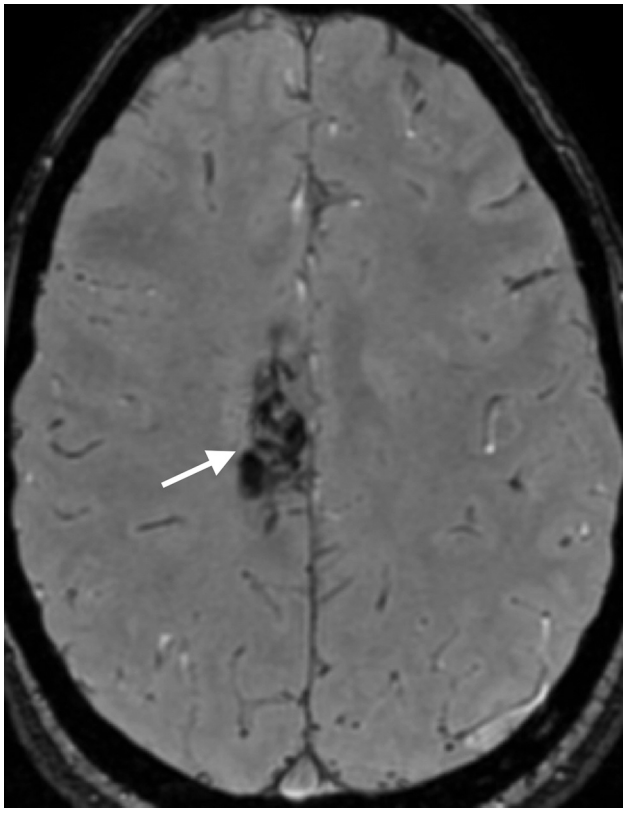

FIG 3. A 19-year-old woman with a right posterior frontal AVM with hemorrhagic presentation, partially embolized with glue. SWAN imaging 2.5 years after SRS shows the complete occlusion of the nidus (*white arrow*) confirmed by DSA (not shown).

callosum AVM with multiple adjacent arteries that gave the impression of hyperintense draining veins (Fig 6). Univariate statistics failed to show any association between false diagnostic results and Spetzler-Martin grade ($P = .6$), AVM location ($P = .6$), previous hemorrhage ($P = 1$), and previous embolization ($P = .27$).

Diagnostic Value of SWAN

The diagnostic accuracy of SWAN for a residual nidus reached a sensitivity of 85.7%, a specificity of 85.7%, a positive predictive value of 85.7%, and a negative predictive value of 85.7%.

DISCUSSION

The role of SWAN in the post-SRS follow-up of bAVMs has not been studied, to our knowledge. Our results show that SWAN has good intermodality (κ = 0.71; 95% CI, 0.45–0.97) and interobserver (κ = 0.64; 95% CI, 0.37–0.92) agreement compared with DSA, with a sensitivity of 85.7%, specificity of 85.7%, positive predictive value of 85.7%, and negative predictive value of 85.7%.

Although SWAN has good diagnostic accuracy, given its actual limitations, a negative SWAN finding cannot assert with certainty whether a bAVM is completely obliterated. However, it may guide imaging follow-up of patients with bAVMs treated with SRS without the need for intravenous injection of gadolinium and may potentially help avoid some unnecessary DSA examinations. After bAVM SRS, SWAN may be performed annually until the findings become negative (ie, until there is no residual shunt visible) and the final result can be confirmed by DSA.

Using SWAN, we found spots of increased signal intensity for residual arteriovenous shunts and patent draining veins in 12 of 14 (85.7%) residual nidi diagnosed by DSA (Fig 2). This hyperintense pattern has been noted in previous SWAN studies of nontreated bAVMs. At high blood velocities, the hypersignal within the nidus and the venous drainage are partially related to an inherent TOF effect of SWAN at 1.5T and 3T.[19,20] At lower blood velocities, higher blood-oxygen levels and a lack of paramagnetic phase shift linked to direct arterial-to-venous shunt inside the nidus appears to be mainly responsible for the hyperintensity.[19]

False-negative diagnoses of a residual nidus on SWAN occurred in 2 cases of residual nidi of millimetric size (Fig 4). False-positive diagnoses of a nidus remnant occurred in 2 patients. In one, a hyperintense signal in a fully occluded nidus was produced by susceptibility artifacts from a large calcified area visible on plain CT (Fig 5). In the other patient, multiple hyperintense normal vessels near the occluded bAVM that proved to be normal arteries gave the false impression of hyperintense small draining veins (Fig 6). This pitfall may be avoided by the use of multiplanar reformations to distinguish draining veins and arteries.[19]

In the present study, 20 of 26 (76.9%) bAVMs had previously bled and contained hemosiderin. However, this was not found to be detrimental to the diagnosis of a residual bAVM nidus ($P = 1$). *n*-BCA glue was used as an embolic agent in 23 of 26 bAVMs before SRS. When injected, *n*-BCA glue is mixed with Lipiodol (Guerbet, Roissy, France), an oil-based contrast agent that could exhibit high signal on T1- and T2-weighted images. However, in the present series, previous embolization was not related to the false diagnosis of a nidus remnant ($P = .27$). One patient had been embolized with Onyx, but the remaining bAVM nidus was correctly diagnosed as patent. Previous embolizations could obscure the margin of the nidus or result in a fragmented nidus and thereby mislead to a false negative diagnosis. Although, in the present series, glue did not interfere with the diagnostic accuracy

Table 2: Detection of nidus remnant on SWAN compared with DSA[a]

	SWAN Reader 1		SWAN Reader 2		Consensus Reading	
DSA	Patent	Obliterated	Patent	Obliterated	Patent	Obliterated
Patent ($n = 14$)	11	3	11	2	12	2
Obliterated ($n = 14$)	5	9	3	12	2	12
Sensitivity (%)	68.7		78.6		85.7	
Specificity (%)	75		85.7		85.7	
PPV (%)	78.6		84.6		85.7	
NPV (%)	64.3		80		85.7	

Note:—PPV indicates positive predictive value; NPV, negative predictive value.
[a] Prevalence of nidus remnant after SRS for bAVM.

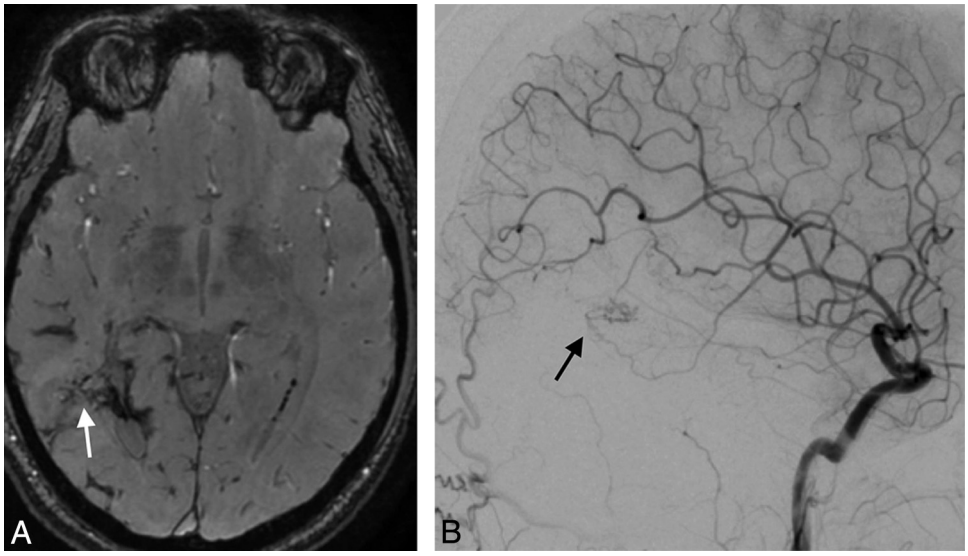

FIG 4. A 32-year-old man with a right parietal AVM with hemorrhagic presentation, partially embolized with glue. SWAN imaging 3.5 years after SRS (*white arrow*, *A*) fails to show a very small residual nidus that was depicted by DSA (*black arrow*, *B*).

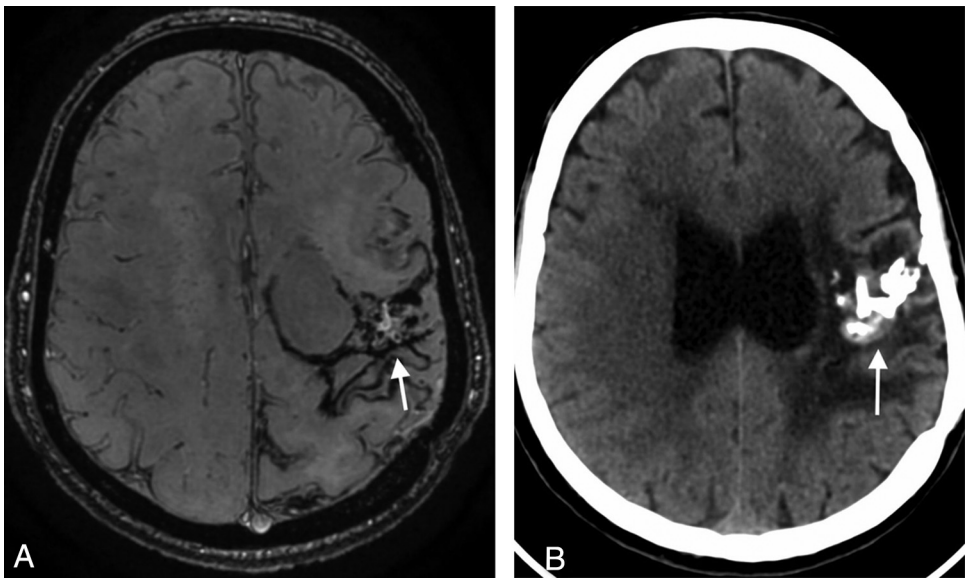

FIG 5. A 60-year-old man with a left parietal AVM with hemorrhagic presentation that was partially embolized with glue. *A*, SWAN imaging 4 years after SRS shows an amorphous area of hyperintensity within the nidus (*white arrow*) that was diagnosed as a nidus remnant, but the DSA findings were negative. *B*, CT shows extensive calcification (*white arrow*) inside the AVM scar.

of SWAN, the potential for diagnostic pitfalls related to the use of ethylene copolymer–based embolic agents should be investigated in larger series.

Lee et al[21] assessed the diagnostic accuracy of 3D-TOF and T1 postcontrast MR imaging for the diagnosis of residual post-SRS treated bAVMs and found sensitivities ranging from 76.7% to 84.9% and specificities from 88.9% to 95%. Other authors have studied the accuracy of time-resolved MRA and have found sen-

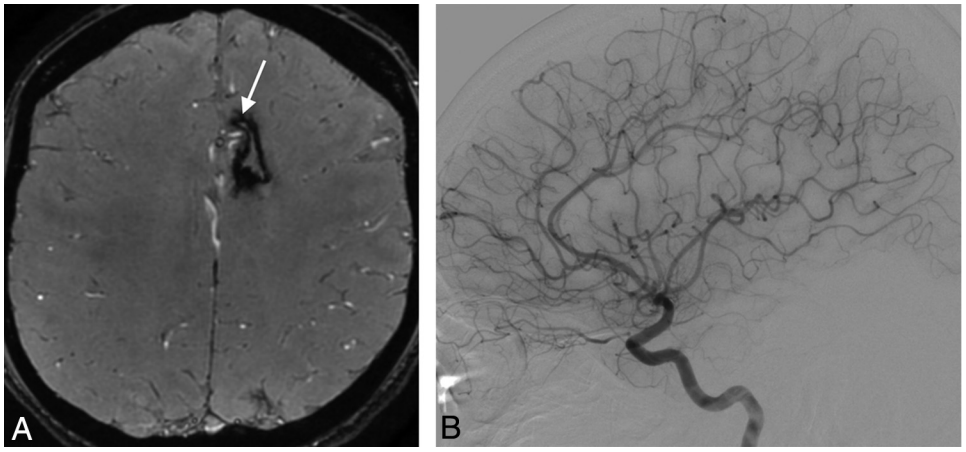

FIG 6. A 19-year-old man with a left frontal AVM with hemorrhagic presentation that was partially embolized with glue. *A*, SWAN imaging 5 years after SRS shows hyperintense vessels (*white arrow*) near the AVM that were mistakenly diagnosed as a nidus remnant. *B*, Digital subtraction angiography findings were negative.

sitivities, specificities, positive and negative predictive values ranging from 64.3% to 79.6%, 90.6% to 100%, 84.6% to 100%, and 78.3% to 90% respectively.[11,21] The clear advantage of SWAN compared to these techniques is the absence of contrast material administration, which represents added cost and entails potential toxicity.[15,16] Compared to 3D-TOF techniques or the detection of T2-weighted flow voids, SWAN has the potential to be more sensitive to small, slow-flow shunts.[19] Nevertheless, a head-to-head comparison with these techniques is warranted.

SWAN is a susceptibility weighted imaging technique available exclusively on GE scanners. Therefore, caution should be used when extrapolating the present findings to susceptibility weighted imaging sequences of other MR imaging machine vendors, where venous drainage may appear hypointense[22-24] or hyperintense.[17,25]

During the study period, a substantial number of patients did not undergo SWAN. This may have introduced bias in our study. Also, studies were performed on MR imaging machines with 2 different field strengths (1.5T and 3T). However, follow-up protocols were consistent. Moreover, readers were not allowed to use MIP or reformatted images, or consult baseline SWAN or DSA studies which, if available, may have improved diagnostic accuracy.

CONCLUSIONS

SWAN is a useful radiation- and contrast material–free technique for the follow-up of patients with brain AVMs treated by SRS. It has the potential to reduce the number of DSA controls after SRS. However, given the actual limitations of SWAN, DSA remains mandatory for the final assessment of brain AVM cure.

REFERENCES

1. Pierot L, Cognard C, Spelle L. **Cerebral arteriovenous malformations: evaluation of the hemorrhagic risk and its morbidity [in French].** *J Neuroradiol* 2004;31:369–75 CrossRef Medline
2. Novakovic RL, Lazzaro MA, Castonguay AC, et al. **The diagnosis and management of brain arteriovenous malformations.** *Neurol Clin* 2013;31:749–63 CrossRef Medline
3. Maruyama K, Kawahara N, Shin M, et al. **The risk of hemorrhage after radiosurgery for cerebral arteriovenous malformations.** *N Engl J Med* 2005;352:146–53 CrossRef Medline
4. Oppenheim C, Meder JF, Trystram D, et al. **Radiosurgery of cerebral arteriovenous malformations: is an early angiogram needed?** *AJNR Am J Neuroradiol* 1999;20:475–81 Medline
5. Steiner L, Lindquist C, Adler JR, et al. **Clinical outcome of radiosurgery for cerebral arteriovenous malformations.** *J Neurosurg* 1992; 77:1–8 CrossRef Medline
6. Dawkins AA, Evans AL, Wattam J, et al. **Complications of cerebral angiography: a prospective analysis of 2,924 consecutive procedures.** *Neuroradiology* 2007;49:753–59 CrossRef Medline
7. Heiserman JE, Dean BL, Hodak JA, et al. **Neurologic complications of cerebral angiography.** *AJNR Am J Neuroradiol* 1994;15:1401–07; discussion 1408–11 Medline
8. Earnest F 4th, Forbes G, Sandok BA, et al. **Complications of cerebral angiography: prospective assessment of risk.** *AJR Am J Roentgenol* 1984;142:247–53 Medline
9. Bendszus M, Koltzenburg M, Burger R, et al. **Silent embolism in diagnostic cerebral angiography and neurointerventional procedures: a prospective study.** *Lancet* 1999;354:1594–97 CrossRef Medline
10. Heidenreich JO, Schilling AM, Unterharnscheidt F, et al. **Assessment of 3D-TOF-MRA at 3.0 Tesla in the characterization of the angioarchitecture of cerebral arteriovenous malformations: a preliminary study.** *Acta Radiol* 2007;48:678–86 CrossRef Medline
11. Lim HK, Choi CG, Kim SM, et al. **Detection of residual brain arteriovenous malformations after radiosurgery: diagnostic accuracy of contrast-enhanced four-dimensional MR angiography at 3.0 T.** *Br J Radiol* 2012;85:1064–69 CrossRef Medline
12. Unlu E, Temizoz O, Albayram S, et al. **Contrast-enhanced MR 3D angiography in the assessment of brain AVMs.** *Eur J Radiol* 2006;60: 367–78 CrossRef Medline
13. Soize S, Bouquigny F, Kadziolka K, et al. **Value of 4D MR angiography at 3T compared with DSA for the follow-up of treated brain arteriovenous malformation.** *AJNR Am J Neuroradiol* 2014;35: 1903–09 CrossRef Medline
14. Hadizadeh DR, Kukuk GM, Steck DT, et al. **Noninvasive evaluation of cerebral arteriovenous malformations by 4D-MRA for preoperative planning and postoperative follow-up in 56 patients: comparison with DSA and intraoperative findings.** *AJNR Am J Neuroradiol* 2012;33:1095–101 CrossRef Medline
15. Kanda T, Ishii K, Kawaguchi H, et al. **High signal intensity in the dentate nucleus and globus pallidus on unenhanced T1-weighted MR images: relationship with increasing cumulative dose of a gadolinium-based contrast material.** *Radiology* 2014; 270:834–41 CrossRef Medline

16. Mawad H, Laurin LP, Naud JF, et al. **Changes in urinary and serum levels of novel biomarkers after administration of gadolinium-based contrast agents.** *Biomark Insights* 2016;11:91–94 CrossRef Medline
17. Jagadeesan BD, Delgado Almandoz JE, Moran CJ, et al. **Accuracy of susceptibility-weighted imaging for the detection of arteriovenous shunting in vascular malformations of the brain.** *Stroke* 2011;42:87–92 CrossRef Medline
18. Hodel J, Rodallec M, Gerber S, et al. **Susceptibility weighted magnetic resonance sequences "SWAN, SWI and VenoBOLD": technical aspects and clinical applications [in French].** *J Neuroradiol* 2012;39:71–86 CrossRef Medline
19. Hodel J, Blanc R, Rodallec M, et al. **Susceptibility-weighted angiography for the detection of high-flow intracranial vascular lesions: preliminary study.** *Eur Radiol* 2013;23:1122–30 CrossRef Medline
20. Schmitz BL, Aschoff AJ, Hoffmann MHK, et al. **Advantages and pitfalls in 3T MR brain imaging: a pictorial review.** *AJNR Am J Neuroradiol* 2005;26:2229–37 Medline
21. Lee KE, Choi CG, Choi JW, et al. **Detection of residual brain arteriovenous malformations after radiosurgery: diagnostic accuracy of contrast-enhanced three-dimensional time of flight MR angiography at 3.0 Tesla.** *Korean J Radiol* 2009;10:333–39 CrossRef Medline
22. Saini J, Thomas B, Bodhey NK, et al. **Susceptibility-weighted imaging in cranial dural arteriovenous fistulas.** *AJNR Am J Neuroradiol* 2009;30:E6 CrossRef Medline
23. Noguchi K, Kuwayama N, Kubo M, et al. **Intracranial dural arteriovenous fistula with retrograde cortical venous drainage: use of susceptibility-weighted imaging in combination with dynamic susceptibility contrast imaging.** *AJNR Am J Neuroradiol* 2010;31:1903–10 CrossRef Medline
24. Gasparetto EL, Pires CE, Domingues RC. **Susceptibility-weighted MR phase imaging can demonstrate retrograde leptomeningeal venous drainage in patients with dural arteriovenous fistula.** *AJNR Am J Neuroradiol* 2011;32:E54 CrossRef Medline
25. Letourneau-Guillon L, Krings T. **Simultaneous arteriovenous shunting and venous congestion identification in dural arteriovenous fistulas using susceptibility-weighted imaging: initial experience.** *AJNR Am J Neuroradiol* 2012;33:301–07 CrossRef Medline